JOURNAL OF CATALYSIS 142, 254–262 (1993)

Carbon Monoxide Removal from Hydrogen-Rich Fuel Cell Feedstreams by Selective Catalytic Oxidation

SE H. OH AND ROBERT M. SINKEVITCH

Physical Chemistry Department, General Motors Research & Development Center, 30500 Mound Road, Box 9055, Warren, Michigan 48090-9055

Received October 6, 1992; revised January 27, 1993

Indirect methanol fuel cells currently being investigated at General Motors for transportation applications require removal of carbon monoxide from the hydrogen-rich gas stream produced by the fuel processing section. A variety of catalytic materials, including noble metals (Pt, Pd, Rh, and Ru) and base metals (Co/Cu, Ni/Co/Fe, Ag, Cr, Fe, and Mn), were evaluated in a laboratory reactor feedstream containing CO, H_2, and O_2 in order to identify alternate catalysts which are more effective than currently used Pt/Al_2O_3 in selectively oxidizing CO in the presence of excess H_2. Both Ru/Al_2O_3 and Rh/Al_2O_3 are among the most active catalysts for CO oxidation, achieving nearly complete CO conversion at temperatures as low as 100°C (compared to ~200°C required for currently used Pt/Al_2O_3). Furthermore, the Ru/Al_2O_3 and Rh/Al_2O_3 catalysts were found to be exceptionally selective for CO oxidation, making it possible to purify the fuel cell feedstream with a minimum loss of the energy content associated with H_2.

INTRODUCTION

Indirect methanol fuel cells are being investigated at General Motors Corporation as a possible energy source for vehicle propulsion and/or auxiliary power units. Since gaseous hydrogen (the most efficient fuel for fuel cells) cannot practically be stored in sufficient quantities aboard a vehicle, it is desirable to integrate a fuel processing section with a fuel cell module for transportation applications (*1–3*). In this self-contained fuel cell system, methanol is converted to hydrogen-rich gas by means of catalytic steam reforming and water–gas shift reaction processes (*4–6*). The product hydrogen is then fed to a hydrogen–air fuel cell that generates electrical power to drive the vehicle. However, the product stream from the fuel processing section (i.e., steam reformer + shifter) typically contains 0.5 to 1 vol% of CO, which severely degrades the fuel cell performance by poisoning the anode oxidation rates. Thus, a viable fuel cell system requires that CO should be removed from the H_2-rich reformed gas down to concentration levels below 0.1 vol% (preferably ~0.01 vol% for extended operation) while minimizing the consumption of H_2.

Possible strategies to accomplish this task include CO removal by adsorption, reduction or oxidation. Among these, selective CO removal by catalytic oxidation (i.e., $CO + 1/2\ O_2 \rightarrow CO_2$) appears to be the most promising approach. Adsorption processes typically require unacceptably large volumes of adsorbents. Reduction steps, such as methanation ($CO + 3H_2 \rightarrow CH_4 + H_2O$), appear attractive; however, the presence of CO_2 in the gas stream severely compromises the processes by generating additional CO as a result of a "shift" of the CO_2. Previous work done at Engelhard Industries (*7*) and Los Alamos National Laboratory (*8*) has shown that Pt/Al_2O_3 catalysts can be effective in selectively oxidizing CO in the presence of excess H_2, but close control of the reactor temperature and the oxygen injection rate is required. Recent efforts in this area have been directed toward improving the selectivity of Pt/Al_2O_3 for CO conver-

0021-9517/93 $5.00

TABLE 1

Characteristics of Catalyst Samples Used

Catalyst	Metal loading (wt%)	BET area (m^2/g)	Source
Pt/Al_2O_3	0.5	184	Matheson, Coleman & Bell
Pd/Al_2O_3	0.5	184	Matheson, Coleman & Bell
Rh/Al_2O_3	0.5	184	Matheson, Coleman & Bell
Ru/Al_2O_3	0.5	184	Matheson, Coleman & Bell
$Co/Cu/Al_2O_3$	5Co/5Cu	59	Harshaw Chemical
$Ni/Co/Fe/Al_2O_3$	3Ni/3Co/3Fe	78	Harshaw Chemical
Ag/Al_2O_3	4	1	Harshaw Chemical
Cr/Al_2O_3	8	63	Harshaw Chemical
Fe/Al_2O_3	14	41	Harshaw Chemical
Mn/SiO_2	1.5	258	Harshaw Chemical

sion in a H_2-rich reformed gas stream through optimization of the design and operation of the "preferential oxidation reactor" (PROX). Among the designs evaluated is a concept of a multiple-stage PROX, where the amount of oxygen injected and the temperature level for each stage are optimized to effectively remove CO while minimizing hydrogen oxidation (*9, 10*).

Another way to improve the performance of the PROX is to employ alternate catalytic materials which are more active and selective than currently used Pt/Al_2O_3 catalysts for CO oxidation in the presence of excess H_2. This approach has the advantage of potentially eliminating the need for complex hardware required for the distributed temperature control and oxygen injection along the length of a multiple-stage Pt/Al_2O_3 catalytic reactor.

This study was initiated to identify catalysts that efficiently and selectively oxidize CO present in the H_2-rich gas stream from the fuel processing unit. A variety of catalytic materials were examined, including noble metals (Pt, Pd, Rh, and Ru) and base metals (Co/Cu, Ni/Co/Fe, Ag, Cr, Fe, and Mn), in laboratory feedstreams containing CO, H_2, and O_2. Particular attention was given to the activities and selectivities of the catalysts for CO oxidation as a function of temperature and oxygen concentration. High CO oxidation activity is desirable because it would allow CO removal at temperatures compatible with the operation of solid-polymer-electrolyte fuel cells (90 to 110°C). Also important is the high selectivity for promoting the $CO–O_2$ reaction versus the $H_2–O_2$ reaction, because it is desired to remove CO from the fuel cell feedstream with a minimum loss of the energy content associated with H_2.

EXPERIMENTAL

Catalysts

A variety of commercially-supplied supported noble metal and base metal catalysts were evaluated in this study. Table 1 lists the metal loadings, BET surface areas, and the source of the catalyst samples used for the reactor experiments. All of the catalysts were in the form of cylindrical pellets (3.2 mm diameter by 3.2 mm length) except for the Mn/SiO_2 catalyst which was supplied as 3.2-mm granules.

Reactor System and Analytical Methods

A schematic diagram of the reactor system is shown in Fig. 1. The reactor was a 2.5-cm-o.d. stainless steel tube housed in an electric furnace. The feed gas was passed downward through the reactor containing stacked layers of SiC pellets (for preheating the gas) and catalyst pellets. The reactor

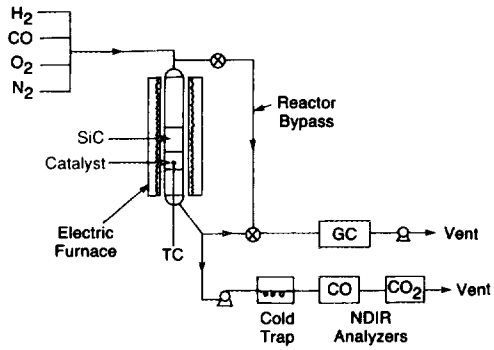

FIG. 1. Schematic diagram of the reactor system.

temperature variations were controlled by a proportional controller to make them consistently repeatable. A stable and linear increase in inlet temperature was obtained with the control thermocouple placed at the outside surface of the reactor tube. However, temperature values quoted in this study (referred to as catalyst temperature) are those actually measured with a chromel–alumel thermocouple located along the reactor centerline in the middle of the catalyst bed.

All the experiments reported here were done using 30 cm^3 of catalyst and a total feedstream flow rate of 10 liter/min (STP), yielding a space velocity of 20,000 h^{-1}. The feedstream contained 0.85 vol% H_2, 900 ppm CO, and 0 to 2300 ppm O_2 in an N_2 background. A nearly tenfold excess of H_2 over CO was employed in order to simulate the H_2-rich gas stream produced by a fuel processing section.

The concentrations of CO, H_2, and O_2 in the reactor inlet and outlet streams were measured with a Varian Model 3400 gas chromatograph equipped with a thermal conductivity detector (TCD). The GC contained a stainless steel column (0.32 cm diameter by 3 m length) packed with Molecular Sieve 5A (60–80 mesh). The column was operated at 60°C for 3 min followed by temperature programming to 70°C at a rate of 5°C/min in order to separate H_2, O_2, N_2, and CO. Both the injector and detector were maintained at 120°C, and the TCD filament temperature was 220°C. Sample injection was accomplished using helium as the carrier gas at a flow rate of 15 cm^3/min. Individual species in the reaction mixture were identified and quantified by comparing their elution times and integrated peak areas with those of calibration gas mixtures of known concentration.

A portion of the reactor effluent (~3 liter/min) was passed through Horiba nondispersive infrared analyzers to continuously measure concentrations of CO and CO_2. These analyzers provided a convenient means of monitoring the catalyst efficiency for CO oxidation as a function of temperature during dynamic temperature run-up experiments.

Oxidation Activity Measurements

Catalytic behavior was characterized in two ways: (1) variable temperature experiments with a fixed feedstream composition, and (2) variable O_2 concentration experiments at a fixed temperature. All the catalysts were stabilized by carrying out repetitive runs of temperature run-up experiments where the catalyst was heated from room temperature to 450°C at a rate of 20°C/min in the flowing feed containing 0.85% H_2, 900 ppm CO, and 800 ppm O_2 (balance N_2). Once stabilized, the catalysts yielded reproducible conversion versus temperature profiles; the 50% CO conversion temperatures obtained during consecutive temperature run-up experiments generally agreed within several degrees. The variable O_2 concentration experiments were done by first heating the sample to 450°C in the above mentioned feedstream, holding steady at 450°C for 15 min, and then cooling down to the desired temperature before varying the feedstream concentration of O_2.

We also made activity measurements without any catalyst in the reactor (i.e., with catalyst replaced with blank alumina pellets). The conversions of CO and H_2 at typical feedstream compositions were found to be insignificant below 300°C. Also, for the

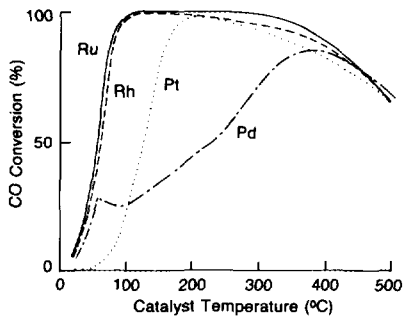

FIG. 2. CO conversion over Ru/Al_2O_3, Rh/Al_2O_3, Pt/Al_2O_3, and Pd/Al_2O_3 during temperature run-up in a feedstream containing 0.85 vol% H_2, 900 ppm CO, and 800 ppm O_2 in an N_2 background.

feedstream composition employed for temperature run-up experiments, the axial temperature gradient through the catalyst bed is estimated to be at most 15°C, indicating that plotting the conversion as a function of mid-bed temperature is adequate to describe the catalytic properties of the sample being tested.

RESULTS

CO Oxidation Activity

Figure 2 compares CO conversion efficiencies measured over the four noble metal catalysts (all 0.5 wt% metal dispersed on alumina pellets) during a temperature run-up in the reactant stream containing 0.85 vol% H_2, 900 ppm CO, and 800 ppm O_2. It is evident from Fig. 2 that both Ru/Al_2O_3 and Rh/Al_2O_3 are most active for CO oxidation, approaching 100% CO conversion at temperatures as low as 100°C. The 50% conversion temperatures for these catalysts are ~70°C lower than that for the Pt/Al_2O_3 catalyst. A rather unusual conversion versus temperature profile was obtained with the Pd/Al_2O_3 catalyst. At low temperatures, the CO oxidation data for Pd/Al_2O_3 closely follows those for Ru/Al_2O_3 and Rh/Al_2O_3, reaching ~25% CO conversion at 60°C. At higher temperatures, however, the CO conversion exhibited a much weaker temperature dependence, diverging sharply from the conversion profiles for Ru/Al_2O_3 and Rh/Al_2O_3. Over the temperature range of interest in PROX operation (100 to 200°C), the CO oxidation activity in the presence of excess H_2 decreases in the order $Ru/Al_2O_3 > Rh/Al_2O_3 > Pt/Al_2O_3 > Pd/Al_2O_3$.

It is interesting to note in Fig. 2 that all four noble metal catalysts exhibit a maximum in the CO conversion with increasing temperature. The decline in CO conversion at elevated temperatures was not due to an irreversible change in the catalysts; the conversion curves during the cool-down followed virtually the same paths as the run-up curves. The observed decrease in CO conversion with temperature appears to be related to the water–gas shift equilibrium limiting the CO conversion at high temperatures (as discussed later), leading to consumption of the limited supply of O_2 in the feed by the H_2 in preference to the CO. It is interesting to note that a temperature run-up experiment with a H_2-free feedstream containing only CO and O_2 did not produce a maximum in the conversion versus temperature curve (see solid line in Fig. 3). The results of Fig. 2 suggest that high-temperature operation of the PROX containing noble metal catalysts is undesirable because H_2 (fuel), rather than CO (impurity), would be preferentially removed by the catalytic oxidation.

The results for various base metal cata-

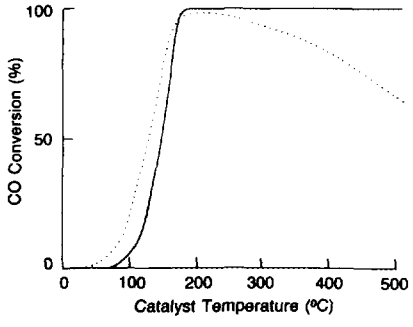

FIG. 3. Comparison of CO conversion versus temperature curves for Pt/Al_2O_3 with (dotted line) and without (solid line) H_2 in the feed. The feed contained 900 ppm CO and 800 ppm O_2 in both cases.

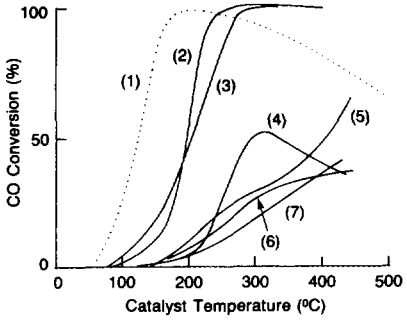

FIG. 4. CO conversion over various base metal catalysts during temperature run-up in a feedstream containing 0.85 vol% H_2, 900 ppm CO, and 800 ppm O_2 in an N_2 background. Data are shown for (1) Pt/Al_2O_3, (2) $Co/Cu/Al_2O_3$, (3) $Ni/Co/Fe/Al_2O_3$, (4) Ag/Al_2O_3, (5) Cr/Al_2O_3, (6) Fe/Al_2O_3, and (7) Mn/SiO_2.

lysts are shown in Fig. 4. For reference, the CO conversion curve for Pt/Al_2O_3 (same data shown in Fig. 2) was also included in the figure. Although the Co-containing catalysts (samples (2) and (3)) exhibited the highest CO oxidation activity of the base metal catalysts examined here, they all performed poorly in comparison to currently used Pt/Al_2O_3 and thus were eliminated from further consideration.

In addition to the temperature effects discussed above, the O_2 concentration in the feed is another important operating variable influencing the performance of the PROX. Figure 5 shows CO conversion versus O_2 concentration data obtained with Ru/Al_2O_3, Rh/Al_2O_3, Pt/Al_2O_3, and Pd/Al_2O_3 in the temperature range where the current PROX typically operates. At a catalyst temperature of 171°C, the Pt/Al_2O_3 catalyst requires 1700 ppm O_2 in the feed in order to achieve complete CO conversion. The Ru/Al_2O_3 and Rh/Al_2O_3 catalysts, on the other hand, reached 100% CO conversion at 800 ppm O_2 at a comparable catalyst temperature of 180°C. The Pd/Al_2O_3 catalyst was much less active than the other three noble metal catalysts; only 70% CO conversion was obtained even in the presence of 2300 ppm O_2 in the feed. In agreement with the results of Fig. 2, the CO oxidation activity in the temperature range characteristic of the operation of the current PROX was found to decrease in the order Ru/Al_2O_3 > Rh/Al_2O_3 > Pt/Al_2O_3 > Pd/Al_2O_3. The same activity ranking was observed during variable O_2 concentration experiments at lower temperatures.

The experiments discussed above demonstrate that Ru/Al_2O_3 and Rh/Al_2O_3 are much more active than currently used Pt/Al_2O_3 for CO oxidation in the presence of excess H_2. Besides their higher CO oxidation activity, Ru/Al_2O_3 and Rh/Al_2O_3 offer the added advantage of consuming substantially smaller amounts of H_2 in the PROX than Pt/Al_2O_3. This aspect is illustrated in Fig. 6, which compares the H_2 conversions measured over the Ru/Al_2O_3, Rh/Al_2O_3, and Pt/Al_2O_3 catalysts

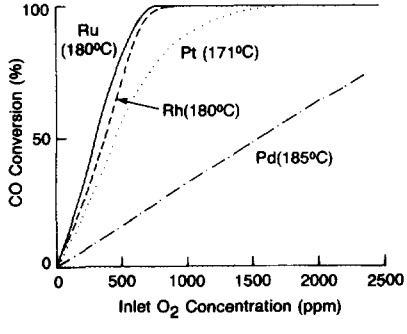

FIG. 5. CO conversion over Ru/Al_2O_3, Rh/Al_2O_3, Pt/Al_2O_3, and Pd/Al_2O_3 in the temperature range 171 to 185°C. The feed contained 0.85 vol% H_2, 900 ppm CO, and variable levels of O_2 in an N_2 background.

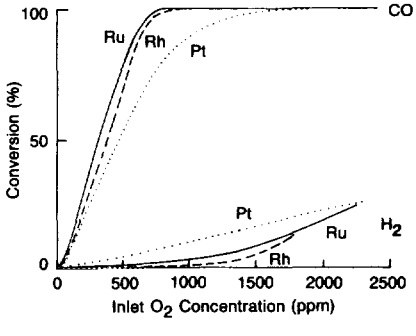

FIG. 6. Conversions of CO and H_2 over Ru/Al_2O_3, Rh/Al_2O_3, and Pt/Al_2O_3 in the temperature range 171 to 180°C. The feed contained 0.85 vol% H_2, 900 ppm CO, and variable levels of O_2 in an N_2 background.

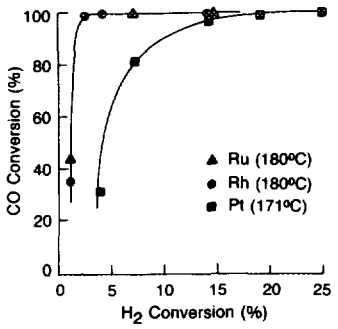

FIG. 7. Comparison of the selectivity of Ru/Al_2O_3, Rh/Al_2O_3, and Pt/Al_2O_3 for the $CO-O_2$ reaction versus the H_2-O_2 reaction in the temperature range 171 to 180°C.

during the same variable O_2 composition experiments of Fig. 5. The CO conversion data of Fig. 5 were reproduced in Fig. 6 for comparison purposes. (The Pd/Al_2O_3 catalyst data are not shown in Fig. 6 in view of its low CO oxidation activity.) Although the tendency to consume H_2 in the presence of CO over the noble metal catalysts decreases in the order $Pt/Al_2O_3 > Ru/Al_2O_3 > Rh/Al_2O_3$, the H_2 conversion over all three catalysts increases monotonically with increasing O_2 concentration. Comparisons of the CO and H_2 conversion curves in Fig. 6 indicate that for each of the noble metal catalysts, there exists an optimum O_2 concentration at which nearly complete CO conversion can be achieved with only limited amounts of H_2 consumed in the PROX. Increasing the O_2 concentration beyond the optimum value would simply increase the extent of H_2 consumption without significantly improving the catalyst efficiency for CO removal from the reformed gas. It is evident in Fig. 6 that Ru/Al_2O_3 and Rh/Al_2O_3 are more effective than Pt/Al_2O_3 in selectively oxidizing CO in the presence of excess H_2; over Pt/Al_2O_3 complete removal of CO is accompanied by at least 20% H_2 conversion, whereas the H_2 conversion over Ru/Al_2O_3 and Rh/Al_2O_3 can be kept below 5% at complete CO conversion.

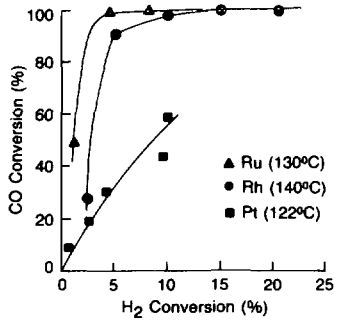

FIG. 8. Comparison of the selectivity of Ru/Al_2O_3, Rh/Al_2O_3, and Pt/Al_2O_3 for the $CO-O_2$ reaction versus the H_2-O_2 reaction in the temperature range 122 to 140°C.

Selectivity

As pointed out in the above discussion, our goal is to remove CO with minimum H_2 consumption, and thus the selectivity (i.e., the partitioning of the limited supply of O_2 between the CO and H_2 present in the reformed gas) is an important factor in the selection of PROX catalysts. The selectivity characteristics of the various noble metal catalysts can be more clearly seen by plotting the data of Fig. 6 in the $CO-H_2$ conversion plane with the O_2 concentration as a parameter. Such a plot is shown in Fig. 7 for the Ru/Al_2O_3, Rh/Al_2O_3, and Pt/Al_2O_3 catalysts in the temperature range of 171–180°C. It is evident that both Ru/Al_2O_3 and Rh/Al_2O_3 possess much stronger preference for the $CO-O_2$ reaction than Pt/Al_2O_3 in the temperature range encountered in the current PROX. Since the higher CO oxidation activity of Ru/Al_2O_3 and Rh/Al_2O_3 would allow us to operate the PROX at lower temperatures (see Fig. 2), it is of interest to compare the low-temperature O_2 partitioning between CO and H_2 for the noble metal catalysts. The selectivity results in the low-temperature range (122–140°C) are presented in Fig. 8. Again, the superior selectivity of Ru/Al_2O_3 and Rh/Al_2O_3 is clearly demonstrated.

DISCUSSION

A great deal of work has been done on the kinetics and mechanism of the $CO-O_2$

reaction [e.g., Refs. (*11–16*)] and the H_2–O_2 reaction [e.g., Refs. (*17–21*)] over noble metal catalysts. Relatively little attention, however, has been given to the simultaneous catalytic oxidation of CO and H_2 in CO–H_2–O_2 mixtures. Although the detailed mechanism of the co-oxidation of CO and H_2 over noble metals is not yet well understood, it has generally been observed that the H_2 oxidation is strongly inhibited by the presence of CO in the reactant stream (*22, 23*). This observation is not surprising in view of the fact that CO is adsorbed much more strongly on noble metal surfaces than H_2 or O_2 (*11, 13, 24*). As a result of its strong adsorption strength, CO would cover the catalyst surface almost entirely, excluding the more weakly adsorbed species, H_2 and O_2, from the active sites in CO–H_2–O_2 mixtures. Consequently, virtually no reaction would occur until the temperature is high enough to desorb significant amounts of CO from the catalyst surface. This situation is very similar to that encountered during CO oxidation in the absence of H_2 (*13, 14*) in that the onset of the reaction both in the presence and absence of H_2 in the feed is controlled by the desorption of CO. This indicates that the lightoff behavior of the noble metal catalysts in CO–H_2–O_2 mixtures is dominated by the kinetic features characteristic of the CO–O_2 reaction rather than by those of the H_2–O_2 reaction.

It should be noted that the abovementioned mechanism represents only an approximation to reality. For example, the presence of H_2 in the reactant stream can give rise to an interaction with adsorbed CO on the surface, such as the formation of an H–CO complex (*24, 25*), resulting in a significant enhancement of CO oxidation activity [see Fig. 3 for $T < 180$°C as well as Refs. (*22, 23*)]. This surface complex is believed to enhance the reaction by desorbing from the catalyst surface below the temperature required for CO desorption in the absence of H_2 (*23*). Nevertheless, the mechanistic discussion given above provides a reasonable description of the essential features of the CO–H_2–O_2 reaction system catalyzed by noble metals. This argument is supported by the same activity ranking for CO oxidation (Ru > Rh > Pt > Pd) observed both in the absence of H_2 (*16*) and in the presence of H_2 (see Figs. 2 and 5) over the temperature range of 100 to 200°C.

Once the reaction is initiated by the onset of CO desorption, the catalyst surface undergoes an abrupt decrease in the surface coverage of CO, resulting in the increased population of available active sites (*26, 27*). In this case the surface is no longer predominantly covered with CO, and thus it is reasonable to speculate that the rate of the H_2–O_2 reaction in CO–H_2–O_2 mixtures during and after catalyst lightoff would not be greatly affected by the CO. This argument is supported by the fact that our observation of substantially higher H_2 conversions over Pt/Al_2O_3 than Rh/Al_2O_3 (Fig. 6) is consistent with the activity ranking reported in the literature for the H_2 oxidation itself (*28*). Literature data on the H_2–O_2 reaction kinetics over Ru is rare; however, Ru is generally believed to be a poor water formation catalyst because of its inability to form stable surface hydroxyl species, a key intermediate in the H_2O formation reaction (*29*).

Figure 2 shows that all four noble metal catalysts exhibit a decline in CO conversion in the regime of high temperatures. The high-temperature CO conversion curves are more or less independent of the catalyst composition. Given the presence of CO, CO_2, H_2, and H_2O in the reaction mixture, it is possible that the product distribution for the CO–H_2–O_2 reaction system at high temperatures may be constrained by the water–gas shift equilibrium. Assuming that all the inlet O_2 is consumed by the reaction, the CO conversion at equilibrium is calculated to be 88% at 250°C, 78% at 350°C, and 60% at 450°C for the feedstream composition considered in Fig. 2. Although these calculated CO conversions are somewhat lower than those actually measured, they correctly describe the trend of CO conversion changes with temperature depicted in

Fig. 2. Possible reasons for the discrepancies between the measured and calculated CO conversion levels include (1) insufficient time for reaching the equilibrium during the temperature run-up, and (2) calculation of the equilibrium constant based on the mid-bed temperature in the presence of a significant temperature gradient within the catalyst bed.

The unusual catalytic behavior of the Pd/Al_2O_3 catalyst shown in Fig. 2 is similar to the complicated conversion versus temperature profiles previously reported for the methanol and formaldehyde oxidation over Pd/Al_2O_3 (*30*). In that earlier work, a local minimum in the conversion versus temperature profile was well described by a kinetic model which allows for a change in the oxidation state of Pd from a reduced (highly active) form to an oxidized (less active) form with increasing temperature. This explanation is reasonable because Pd is known to have a low heat of formation for the metal oxide (i.e., PdO) relative to other noble metals.

Thus, we propose the following intepretation of the unusual conversion versus temperature profile observed in Fig. 2 for the $CO–H_2–O_2$ reaction system catalyzed by the Pd/Al_2O_3 catalyst. Below ~60°C, the Pd is fully reduced and the conversion increases in normal fashion with temperature. As the temperature is increased further, the catalyst begins to oxidize and the conversion falls due to a lower activity of the oxidized Pd compared to the reduced Pd. The conversion reaches a local minimum at ~90°C, where the catalyst is nearly fully oxidized. Above 90°C, the conversion increases again reflecting an activated reaction process characteristic of the oxidized Pd.

REFERENCES

1. Springer, T. E., Murray, H. S., and Vanderborgh, N. E., "Methanol Reformer System and Design for Electrical Vehicles." Presented at 20th Intersociety Energy Conversion Engineering Conference, Miami Beach, FL, August 18–23, 1985.
2. Springer, T. E., Murray, H. S., and Vanderborgh, N. E., "On-Board Fuel Processing for Electric Vehicles." Presented at the Fuel Cell Seminar, Tucson, AZ, May 19–22, 1985.
3. Vanderborgh, N. E., Springer, T. E., and Huff, J. R., "Fuel Processor for Fuel Cell Power System." U.S. Patent No. 4,650,727 (March 17, 1987).
4. Amphlett, J. C., Evans, M. J., Jones, R. A., Mann, R. F., and Weir, R. D., *Can. J. Chem. Eng.* **59,** 720 (1981).
5. Amphlett, J. C., Evans, M. J., Mann, R. F., and Weir, R. D. *Can. J. Chem. Eng.* **63,** 605 (1985).
6. Santacesaria, E., and Carra, S., *Appl. Catal.* **5,** 345 (1983).
7. Cohn, J. G. E., "Process for Selectively Removing Carbon Monoxide from Hydrogen-Containing Gases." U.S. Patent 3,216,783 (November 1965).
8. Vlastnik, V. J., Armellini, F. J., and Jordano, F. A., "Carbon Monoxide Removal by Preferential Oxidation from Hydrogen-Rich Gas Streams." Los Alamos Station, School of Chemical Engineering Practice, Massachusetts Institute of Technology, August 1987.
9. Vanderborgh, N. E., Nguyen, T. V., and Guante, J., "Device for Staged Carbon Monoxide Oxidation." U.S. Patent filed, Invention No. G-2848 (August 1988).
10. Nguyen, T. V., Vanderborgh, N. E., and Guante, J., unpublished results, Los Alamos National Laboratory, Los Alamos, NM, 1988.
11. Engel, T., and Ertl, G., "Advances in Catalysis" (W. G. Frankenburg, V. I. Komarewsky, and E. K. Rideal, Eds.). Vol. 28, p. 1. Academic Press, New York, 1979.
12. Campbell, C. T., Shi, S.-K., and White, J. M., *Appl. Surf. Sci.* **2,** 382 (1979).
13. Oh, S. H., Fisher, G. B., Carpenter, J. E., and Goodman, D. W., *J. Catal.* **100,** 360 (1986).
14. Berlowitz, P. J., Peden, C. H. F., and Goodman, D. W., *J. Phys. Chem.* **92,** 5213 (1988).
15. Peden, C. H. F., and Goodman, D. W., *J. Phys. Chem.* **90,** 1360 (1986).
16. Cant, N. W., Hicks, P. C., and Lennon, B. S., *J. Catal.* **54,** 372 (1978).
17. Acres, G. J. K., *Platinum Met. Rev.* **10,** 60 (1966).
18. Hanson, F. V., and Boudart, M., *J. Catal.* **53,** 56 (1978).
19. Gland, J. L., Fisher, G. B., and Kollin, E. B., *J. Catal.* **77,** 263 (1982).
20. Hellsing, B., Kasemo, B., Ljungstrom, S., Rosen, A., and Wahnstrom, T., *Surf. Sci.* **189/190,** 851 (1987).
21. Fisher, G. B., and DiMaggio, C. L., "The Observation of Stable Hydroxyl Formation by Hydrogen Addition to Adsorbed Oxygen on Rh (100)." Presented at 10th N. Am. Mtg. Catal. Soc., San Diego, CA, May 18, 1987; General Motors Research Publication GMR-5596.

22. Dabill, D. W., Gentry, S. J., Holland, H. B., and Jones, A., *J. Catal.* **53,** 164 (1978).
23. Stetter, J. R., and Blurton, K. F., *Ind. Eng. Chem. Prod. Res. Dev.* **19,** 214 (1980).
24. Nishiyama, Y., and Wise, H., *J. Catal.* **32,** 50 (1974).
25. Baldwin, V. H., and Hudson, J. B., *J. Vac. Sci. Technol.* **8,** 49 (1971).
26. Herz, R. K., and Marin, S. P., *J. Catal.* **65,** 281 (1980).
27. Golchet, A., and White, J. M., *J. Catal.* **53,** 266 (1978).
28. Golodets, G. I., "Heterogeneous Catalytic Reactions Involving Molecular Oxygen," Studies in Surface Science and Catalysis, Vol. 15, Chap. IX. Elsevier, Amsterdam, 1983.
29. Thiel, P. A., and Madey, T. E., *Surf. Sci. Rep.* **7,** 211 (1987).
30. McCabe, R. W., and Mitchell, P. J., *Appl. Catal.* **44,** 73 (1988).